Aalborg Universitet

AALBORG UNIVERSITY
DENMARK

Identification of the Skirt Piled Gullfaks C Gravity Platform using ARMAV Models

Kirkegaard, Poul Henning; Andersen, P.; Brincker, Rune

Publication date:
1995

Document Version
Publisher's PDF, also known as Version of record

Link to publication from Aalborg University

Citation for published version (APA):
Kirkegaard, P. H., Andersen, P., & Brincker, R. (1995). *Identification of the Skirt Piled Gullfaks C Gravity Platform using ARMAV Models*. Dept. of Building Technology and Structural Engineering, Aalborg University. Fracture and Dynamics Vol. R9534 No. 69

General rights
Copyright and moral rights for the publications made accessible in the public portal are retained by the authors and/or other copyright owners and it is a condition of accessing publications that users recognise and abide by the legal requirements associated with these rights.

- Users may download and print one copy of any publication from the public portal for the purpose of private study or research.
- You may not further distribute the material or use it for any profit-making activity or commercial gain
- You may freely distribute the URL identifying the publication in the public portal -

Take down policy
If you believe that this document breaches copyright please contact us at vbn@aub.aau.dk providing details, and we will remove access to the work immediately and investigate your claim.

Downloaded from vbn.aau.dk on: April 20, 2024

INSTITUTTET FOR BYGNINGSTEKNIK
DEPT. OF BUILDING TECHNOLOGY AND STRUCTURAL ENGINEERING
AALBORG UNIVERSITET • AUC • AALBORG • DANMARK

Aalborg Universitetsbibliotek
530005198320

FRACTURE & DYNAMICS
PAPER NO. 69

To be presented at the 14th International Modal Analysis Conference
Dearborn, Michigan, USA, February 12-15, 1996

P. H. KIRKEGAARD, P. ANDERSEN & R. BRINCKER
IDENTIFICATION OF THE SKIRT PILED GULLFAKS C GRAVITY PLATFORM USING ARMAV MODELS

DECEMBER 1995 ISSN 1395-7953 R9534

The FRACTURE AND DYNAMICS papers are issued for early dissemination of research results from the Structural Fracture and Dynamics Group at the Department of Building Technology and Structural Engineering, University of Aalborg. These papers are generally submitted to scientific meetings, conferences or journals and should therefore not be widely distributed. Whenever possible reference should be given to the final publications (proceedings, journals, etc.) and not to the Fracture and Dynamics papers.

Printed at Aalborg University

INSTITUTTET FOR BYGNINGSTEKNIK
DEPT. OF BUILDING TECHNOLOGY AND STRUCTURAL ENGINEERING
AALBORG UNIVERSITET • AUC • AALBORG • DANMARK

FRACTURE & DYNAMICS
PAPER NO. 69

To be presented at the 14th International Modal Analysis Conference
Dearborn, Michigan, USA, February 12-15, 1996

P. H. KIRKEGAARD, P. ANDERSEN & R. BRINCKER
IDENTIFICATION OF THE SKIRT PILED GULLFAKS C GRAVITY PLATFORM USING ARMAV MODELS

DECEMBER 1995 ISSN 1395-7953 R9534

IDENTIFICATION OF THE SKIRT PILED GULLFAKS C GRAVITY PLATFORM USING ARMAV MODELS

P.H. Kirkegaard, P. Andersen & R. Brincker
Aalborg University
Department of Building Technology and Structural Engineering
Sohngaardsholmsvej 57, DK-9000 Aalborg, Denmark

ABSTRACT

This paper presents the results from the system identification of the Gullfaks C gravity offshore platform excited by natural loads. The paper describes how modal parameters and mode shapes can be estimated by use of ARMAV models. The results estimated by an ARMAV model are compared with results estimated by an ARV model which can be interpreted as a truncated ARMAV model. The results show the usefulness of the approaches for identification of offshore structures excited by natural excitation.

NOMENCLATURE

M	Mass matrix
K	Stiffness matrix
C	Damping matrix
$x(t)$	Displacement vector
$z(t)$	State vector
t	Time
A	State transition matrix
B	Input matrix
ζ_j	Damping ratio of the jth mode
ω_j	Natural angular eigen-frequency of the jth mode
Δ	Sampling period
U	Continuous-time eigenvector matrix
μ	Continuous-time eigenvalue matrix
X_k	Discrete-time system response
A_i	Auto-regressive matrices
B_j	Moving-average matrices
a_k	Discrete-time white noise
Z_k	Discrete-time state vector
F	Discrete-time state space matrix
W_k	Discrete-time excitation matrix
L	Discrete-time eigenvector matrix
λ	Discrete-time eigenvalue matrix

1. INTRODUCTION

Since the end of the sixties the interest in the system identification based on time domain models has increased, and now literature on system identification is very much dominated by time domain methods. In Ljung [1] and Söderström et al. [2] the basic features of system identification based on time and frequency domain approaches are highlighted. For many years the identification techniques based on scalar auto-regressive moving average (ARMA) models in the time domain have attracted limited interest concerning structural engineering applications. A factor contributing to this situation is that ARMA models have been developed primarily by control engineers and applied mathematicians. Further, ARMA models have been primarily developed concerning systems for which limited a priori knowledge is available, whereas the identification of structural systems relies heavily on understanding of physical concepts. The structural time domain identification techniques using ARMA representation have been compared with frequency domain techniques in e.g. Davies et al. [3]. In this and other papers it has been documented that these ARMA time domain modelling approaches are superior to Fourier approaches for the identification of structural systems since e.g. leakage and resolution bias problems are avoided. These founds make identification techniques utilizing ARMA algorithms interesting for modal parameter estimation. Especially, with respect to damage detection where modal parameters are used as damage indicators. However, in recent years the application of scalar ARMA models as well as a vector ARMA models (ARMAV) to the description of structural systems subjected to ambient excitation has become more common, see e.g. Gersch et al. [4], Pandit et al. [5], Hac et al. [6], Kozin et al. [7], Jensen [8], Safak [9], Hamamonton et al. [10], Li et al. [11], Hoen [12] , Langen [13], Prevosto et al. [14], Pi et al. [15], Piombo et [16] and Andersen et al. [17]. Some of these references have considered identification of offshore structures using different implementation approaches of the ARMA models such as the Modified Yule-Walker approach, see e.g. Hamamonton et al. [10] and Li et al. [11], and the Instrumental Variable approach, see e.g. Prevosto et al. [14] and Hoen [12]. These approaches imply that the identification is based on estimating the autocovarinace functions. However, in this paper the idea is to estimate the modal parameters and mode shapes by calibrating multivariate ARMAV and ARV models directly to the measured response data.

2.THEORY

This section describes the relationship between an Auto-Regressive Moving-Average Vector model (ARMAV) and the governing differential equation for a linear n-degree of freedom elastic system. Further, it is described how an ARV model can be interpreted as a truncated ARMAV model.

2.1 Continuous Time Model

In the continuous time domain an *n*-degree linear elastic viscous damped vibrating system is described to be a system of linear differential equations of second order with a constant coefficient given by a mass matrix M (n x n), a damping matrix C (n x n), a stiffness matrix K (n x n), an input matrix S *(n x r)* and a force vector f(t) (r x 1). Then the equations of motion for a linear multivariate system may in the time domain be expressed as

$$M\ddot{x}(t) + C\dot{x}(t) + Kx(t) = Sf(t) \qquad (1)$$

$x(t)$ is the displacement vector. By introducing the state vector $z(t)$

$$\dot{z}(t) = \begin{bmatrix} x(t) \\ \dot{x}(t) \end{bmatrix} \qquad (2)$$

the dynamic equation (1) can be written into the state-space model in the following way

$$\dot{z}(t) = Ax(t) + Bf(t) \qquad (3)$$

where the system matrix A and the input matrix B are defined by

$$A = \begin{bmatrix} 0 & I \\ -M^{-1}K & -M^{-1}C \end{bmatrix} \quad B = \begin{bmatrix} 0 \\ -M^{-1}S \end{bmatrix} \qquad (4)$$

The solution of the above equation (1) is now given by

$$z(t) = e^{At}z(0) + \int_0^t e^{A(t-\tau)}Bf(\tau)d\tau \qquad (5)$$

It is assumed that the matrix A can be eigenvector-eigenvalue decomposed as

$$A = U\mu U^{-1} \qquad (6)$$

$$U = \begin{bmatrix} u_1 & \cdots & u_{2n} \\ \mu_1 u_1 & \cdots & \mu_{2n}u_{2n} \end{bmatrix} \qquad (7)$$

$$\mu = diag\,[\mu_i] \;,\; i=1,2,...,2n \qquad (8)$$

Φ is the matrix which columns are the scaled mode shapes ϕ_i of the ith mode. Θ is the continuous time diagonal eigenvalue matrix which contains the poles of the system from which the natural frequency ω_i and the damping ratio ζ_i of the ith mode can be obtained for under damped systems from a complex conjugate pair of eigenvalues as

$$\mu_i, \mu_i^* = -\omega_i\zeta_i \pm \omega_i\sqrt{1-\zeta_i^2} \qquad (9)$$

The solution (5) can now be written

$$z(t) = Ue^{\mu t}U^{-1}x(0) + \int_0^t Ue^{\mu(t-\tau)}U^{-1}Bf(\tau)d\tau \qquad (10)$$

2.2 Discrete Time ARMAV Model

For multi variate time series, described by an m-dimensional vector X_k, an ARMAV(p,q) model can be written with p AR-matrices and q MA-matrices

$$X_k + \sum_{i=1}^{p} A_i X_{k-i} = \sum_{j=1}^{q} B_j a_{k-j} + a_k \qquad (11)$$

where the discrete-time system response is $X_k = [X_{k1}, X_{k2} \ldots X_{km}]^T$. A_i is an $m \times m$ matrix of auto-regressive coefficients and B_j is an $m \times m$ matrix, containing the moving-average coefficients. $\mathbf{a}_k$ is the model residual vector, an m-dimensional white noise vector function of time. $k=t/\Delta$ where Δ is the discrete sampling interval. Theoretically, an ARMAV model is equivalent to an ARV model with infinite order. However, if the high order parameters are very small, and they can be neglected, a truncated ARV(p) model can be used to approximate the ARMAV model

$$X_k + \sum_{i=1}^{p} A_i X_{k-i} = a_k \qquad (12)$$

The ARV is often preferred because of the linear procedure of the involved parameter estimation. The parameter estimation of the ARMAV model is a non-linear least squares procedure and requires some skill as well as large computation effort, see e.g. Pandit et al. [5].

A discrete state-space equation for equations (11) or (12) obtained by uniformly sampling the structural responses at time k is given by

$$Z_k = FZ_{k-1} + W_k \tag{13}$$

with the state vector

$$Z_k = \{X_k^T \; X_{k-1}^T \; X_{k-2}^T \; \ldots \; X_{k-p+1}^T\}^T \tag{14}$$

and the discrete system matrix is

$$F = \begin{bmatrix} -A_1 & -A_2 & \ldots & -A_{p-1} & -A_p \\ I & 0 & \ldots & 0 & 0 \\ 0 & I & \ldots & 0 & 0 \\ . & . & \ldots & . & . \\ 0 & 0 & \ldots & I & 0 \end{bmatrix} \tag{15}$$

W_k includes the MA terms for the ARMAV model and the white noise terms for the ARV model, respectively. Assuming $Z_k = Z_0$ and $W_k = 0$ for $k = 0$ implies that the solution of (13) is given by

$$\begin{aligned} Z_k &= F^k Z_0 + \sum_{j=0}^{k-1} F^j W_{k-j} \\ &= L\lambda^k L^{-1} Z_0 + \sum_{j=0}^{k-1} L\lambda^j L^{-1} W_{k-j} \end{aligned} \tag{16}$$

where it is assumed that F can be modal decomposed as

$$F = L\lambda L^{-1} \tag{17}$$

$$\lambda = diag\,[\lambda_i] \;,\; i=1,2,\ldots,pm \tag{18}$$

$$L = \begin{bmatrix} l_1\lambda_1^{p-1} & l_2\lambda_2^{p-1} & \ldots & l_{pm}\lambda_{pm}^{p-1} \\ l_1\lambda_1^{p-2} & l_2\lambda_2^{p-2} & \ldots & l_{pm}\lambda_{pm}^{p-2} \\ . & . & . & . \\ l_1 & l_2 & \ldots & l_{pm} \end{bmatrix} \tag{19}$$

The discrete state space model can now be used to identification of modal parameters and mode shapes as follows. First, the discrete system matrix F is estimated by calibrating (13) to observed data. Next the discrete eigenvalues of F are estimated by solving the eigen-problem $\det(\mathbf{F}-\lambda\mathbf{I}) = 0$ which gives the pm discrete eigenvalues λ_i.The continuous eigenvalues can now be obtained by $\lambda_i = e^{\mu_i \Delta}$ which implies that the modal parameters can be estimated using (9). The mode shapes are determined directly from the columns of the bottom $m \times pm$ submatrix of L. It is seen that the number of discrete eigenvalues in general are larger or different from the number of continuous eigenvalues. Therefore, only a subset of the discrete eigenvalues will be structural eigenvalues. This means that the user has to separate the physical modes from the computational modes. The computational modes are related to the unknown excitation and the measurement noise processes. The separation can often be done by studying the stability of e.g. frequencies, damping ratios and mode shapes, respectively for increasing AR model order. Often, it is also possible to separate the modes by selecting physical modes as the modes with corresponding damping ratios below a reasonable limit for the modal damping ratios.

However, satisfactory results obtained using ARMAV or ARV models for system identification require that appropriate models are selected and validated. Model selection involves the selection of the form and the order of the models, and constitutes the most important part of the system identification. Model validation is to confirm that the model estimated is a realistic approximation of the actual system. Model validation is the final stage of the system identification procedure. Since the system identification is an iterative process various stages will not be separated: models are estimated and the validation results will lead to new models etc. One of the dilemmas in the model validation is that there are many different ways to determine and compare the quality of the estimated models. First of all, the subjective judgement in the model validation should be stressed. It is the user that makes the decision based on numerical indicators. The variance of the parameter estimates can be such an indicator. It is also important to check whether the model is a good fit for the data recording to which it was estimated. Simulation of the system with the actual input and comparing the measured output with the simulated model output can also be used for model validation. One can also compare the estimated transfer function with one estimated by FFT. Statistical tests of the prediction errors are also typically used numerical indicators in model validation. A throughout description of the problem of model selection and validation is given in e.g. Ljung [1] and Söderström [2]. It should be mentioned that a covariance equivalent model is obtained, if the model section and validation show that an ARMAV $(2r, 2r-1)$ model is appropriated, see e.g. Andersen et al. [17], where $r = n/m$, i.e. r is equal to the degree of freedom divided by number of channels.

3. EXAMPLE

In this section the ARMAV and the ARV system identification techniques are used to identify the Gullfaks C platform. Implementation of the computational aspects was done in MATLAB, see PC-MATLAB [18]. These aspects are described in details in Andersen et al. [17]

3.1 Description of The Gullfaks C Gravity Platform

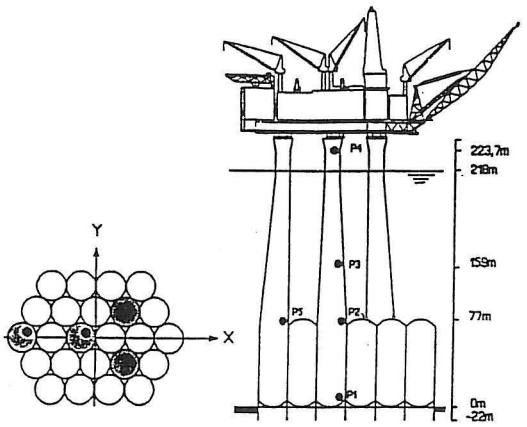

Figure 1: Elevation of the Gullfaks C Platform, Hoen [12].

The considered platform, figure 1, was installed in May 1989 on 220 meters water depth in the North Sea, and was so far the largest and heaviest offshore gravity base concrete structure in the world. The platform was equipped with an extensive instrumentation system for structural, foundation and environmental monitoring, see e.g. Myrvoll [19]. The dynamic motions were measured by means of 15 extremely sensitive linear and angular accelerometers. 13 of the accelerometers are located in the so-called utility shaft at different levels as indicated in figure 1. Two accelerometers recording accelerations in X and Y direction are placed at mudlevel (P1), at cell top level (P2), at the midpoint of the utility shaft (P3) and at the top of the utility shaft (P4), respectively. Further, two angular accelerometers are placed at location P3 and P4, respectively. The accelerations were sampled at 8 Hz during 20 minutes recording periods, giving time series of 9600 samples for each channel. In this paper 3 recording periods have been considered

A : 891226-0100, Hs = 7.8 m, Tp = 11.7 s.
B : 900101-0840, Hs = 3.8 m, Tp = 20.5 s.
C : 900108-0540, Hs = 4.3 m, Tp = 9.6 s

The description of recording period A shows that the data were sampled December 26 1989 where the waves had a significant wave height Hs=7.8 m and a wave peak period Tp = 11.7 s.

In order to investigate the frequency content in the measured time series the FFT autospectrum of the time series has been considered. Figure 2 shows an FFT autospectrum of a time series from recording period A.

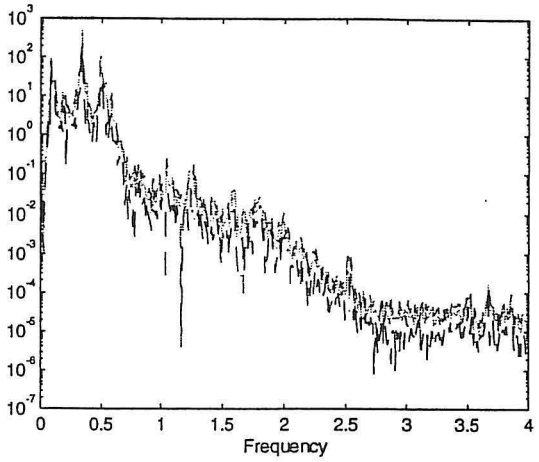

Figure 2: FFT autospectrum with 95% confidence levels

Figure 2 does not show any significant dynamically amplified response above 2 Hz. The same conclusion can be done for the other time series from recording periods A, B and C, respectively. Therefore, prior to the system identification, the data were resampled to 4 Hz. Before the decimation the record was low-pass filtered beyond the new Nyquist frequency. In the following only the two time series from the linear accelerometers at location P2, P3 and P4, respectively, have been used for the identification, i.e. 6 time series have been considered.

3.2 Determination of model order

The order of the ARMAV and ARV models, respectively were selected by incorporating the so-called FPE criteria, see e.g. Ljung [1]. Figure 3 shows the FPE criteria obtained by using the ARMAV and the ARV models on the six selected channels from recording period A.

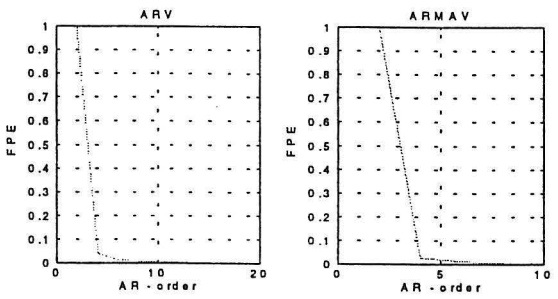

Figure 3: FPE criteria for ARMAV and ARV models

From figure 3 it is seen that only small improvements in the FPE criteria are obtained for an ARMAV(6,5) model with 6 AR terms and an ARV(8) with 8 AR terms. This means that the 36 eigenvalues will be estimated by the ARMAV(6,5) and 48 by the ARV (8), respectively. However only a subset of these eigenvalues belongs to physical modes. Therefore, these have to be separated. The separation can often be done by studying the stability of e.g. frequencies, damping ratios and mode shapes, respectively, for increasing AR model order. Figures 4 and 5 show stabilization

diagrams obtained by the ARV and ARMAV models used on data from recording period A. These diagrams show all the frequencies estimated for increasing AR model order (•). Further, stabilized frequencies, i.e. frequencies with a relative change below 2 per cent from one estimation to another are shown (+). Additionally, the frequencies with a corresponding damping ratio below 10 per cent are presented (o). The stabilization of the mode shapes have not been considered.

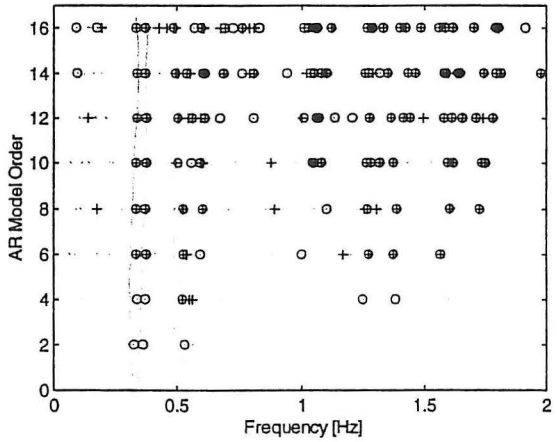

Figure 4: Stabilization diagram for ARV model.

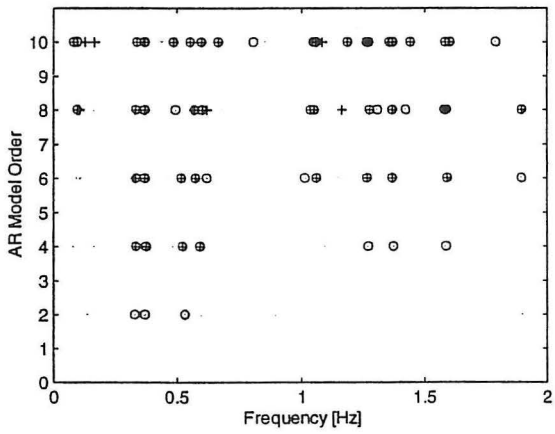

Figure 5: Stabilization diagram for ARMAV model

The stabilization diagrams in figures 4 and 5, respectively show two physical modes just below 0.4. Physical modes are also indicated at approximately 0.5 Hz , 0.6 Hz, 1.0 Hz, 1.26 Hz , 1.4 Hz and 1.6 Hz, respectively. By comparing figures 4 and 5, it is also seen that the ARV and ARMAV models, respectively , estimate the same physical modes. The stabilization diagrams also give an important indication about the order of the models to be used for the parameter estimation process. Based on the results in figures 3, 4 and 5, respectively an ARV(12) and an ARMAV(6,5) are found to be appropriated. The higher order of the ARV model is selected based on the results presented in figure 4. Here it is seen that the stable frequencies at approximately 0.6 Hz are indentified for an ARV(12) model.

After the models are selected the next step is to check the validity of the models. The match of the power spectrum obtained by an FFT and the spectrum obtained from the ARMAV model and the ARV model, respectively ,could be used. Another possiblity is to investigate the residuals. In order to have a valid identification, the residuals should be a white-noise sequence. The plot of the spectrum and autocorrelation of the residual time series from one channel are shown given in figure 6 for the ARV model, respectively.

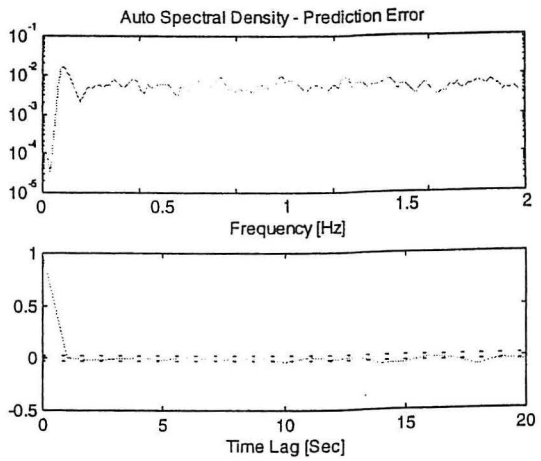

Figure 6: Autospectrum and correlation function of the residuals from one channel estimated by an ARV(12) model.

Visual inspection of the spectrum in figure 6 suggests that the residuals are close to a white-noise sequence, since the peaks are distributed in all frequencies. A more accurate check is to test the autocorrelation of the residuals Two straight lines in figure 6 show the 99% confidence level. For model validity, i.e. whiteness of residuals, the autocorrelation should not exceed these levels, except at zero lag. Figure 6 shows that the autocorrelation remains, for the most part, within the limits, and therefore validate the model. The same conclusions have been stated for all the time series form recording periods A,B and C, respectively.As a final test for model validity, a comparison of model output with recorded output could be performed. This is a more strict test than the previous ones. However, due to space this is not shown here.

3.3 System Identification Results

In this section the estimated modal parmaters and mode shapes are presented and discussed for the first 6 modes. The selected modes are selected based on the conclusions in section 3.2. By comparing stabilization diagrams from all the recording periods the mode with a frequency at approximately 1.0 Hz has been considered to be too unstable to be characterized as a physical mode. Figures 7 and 8 present the estimated modal parameters, respectively, while the figures 9 and 10, respectively , present the magnitude and phase of the mode shapes

Mode		A	B	C
1	f (Hz)	0.333	0.331	0.330
	(%)	0.015	0.013	0.021
2	f (Hz)	0.368	0.371	0.369
	ζ (%)	0.014	0.014	0.013
3	f (Hz)	0.486	0.497	0.491
	ζ (%)	0.033	0.036	0.027
4	f (Hz)	0.572	0.586	0.589
	ζ (%)	0.049	0.054	0.065
5	f (Hz)	0.599	0.622	0.599
	ζ (%)	0.060	0.065	0.075
6	f (Hz)	1.266	1.273	1.266
	ζ (%)	0.018	0.012	0.017

Figure 7: Estimated frequencies and damping ratios using an ARV(12) for recording periods A,B and C, respectively.

Mode		A	B	C
1	f (Hz)	0.336	0.332	0.332
	ζ (%)	0.021	0.016	0.013
2	f (Hz)	0.371	0.373	0.371
	ζ (%)	0.014	0.014	0.015
3	f (Hz)	0.482	0.498	0.493
	ζ (%)	0.045	0.025	0.024
4	f (Hz)	0.556	0.580	0.580
	ζ (%)	0.091	0.088	0.049
5	f (Hz)	0.602	0.618	0.590
	ζ (%)	0.083	0.091	0.104
6	f (Hz)	1.269	1.272	1.260
	ζ (%)	0.024	0.014	0.016

Figure 8: Estimated frequencies and damping ratios using an ARMAV(6,5) for recording periods A,B and C, respectively.

Mode	A: Mag.(Phase)	B: Mag. (Phase)	C: Mag. (Phase)
1-P4-Y	1.000 (0.0)	1.000 (0.0)	1.000 (0.0)
1-P4-X	0.111 (177.1)	0.061 (-133.2	0.078 (214.3)
1-P3-Y	0.375 (-0.07)	0.374 (0.3)	0.375 (0.263)
1-P3-X	0.032 (175.5)	0.019 (-98.1)	0.022 (235.1)
1-P2-Y	0.098 (181.1)	0.097 (-178.9	0.096 (181.0)
1-P2-X	0.006 (171.2)	0.004 (-106.8)	0.005 (231.2)
2-P4-Y	0.064 (-68.9)	0.034 (-38.4)	0.072 (-6.3)
2-P4-X	1.000 (0.0)	1.000 (0.0)	1.000 (0.0)
2-P3-Y	0.023 (-91.6)	0.008 (-97.1)	0.014 (-16.7)
2-P3-X	0.398 (-0.4)	0.397 (-0.3)	0.397 (0.4)
2-P2-Y	0.007 (96.2)	0.002 (105.9)	0.005 (170.9)
2-P2-X	0.089 (-1.8)	0.091 (-1.4)	0.088 (1.4)
3-P4-Y	1.000 (0.0)	1.000 (0.0)	1.000 (0.0)
3-P4-X	0.067 (-86.6)	0.027 (-67.18)	0.029 (-206.5)
3-P3-Y	0.951 (-9.1)	0.955 (1.2)	0.963 (3.6)
3-P3-X	0.148 (-134.3)	0.009 (-168.1)	0.112 (-208.1)
3-P2-Y	0.585 (182.7)	0.587 (-174.8)	0.550 (-172.2)
3-P2-X	0.045 (-140.4)	0.021 (-134.7)	0.045 (-201.1)
4-P4-Y	1.000 (0.0)	1.000 (0.0)	1.000 (0.0)
4-P4-X	0.136 (123.4)	0.237 (-202.3)	0.342 (-255.3)
4-P3-Y	0.270 (134.7)	0.253 (-211.8)	0.094 (-211.7)
4-P3-X	0.111 (88.5)	0.083 (-167.3)	0.086 (-214.4)
4-P2-Y	0.459 (-21.9)	0.397 (-9.0)	0.416 (-5.9)
4-P2-X	0.050 (118.3)	0.049 (-57.3)	0.081 (-134.2)
5-P4-Y	0.914 (-194.1)	0.130 (259.0)	0.522 (-279.0)
5-P4-X	1.000 (0.0)	0.693 (170.9)	1.000 (0.0)
5-P3-Y	0.172 (-23.1)	0.255 (77.7)	0.064 (-189.6)
5-P3-X	0.476 (-220.8)	1.000 (0.0)	0.371 (-90.6)
5-P2-Y	0.292 (-180.5)	0.129 (239.8)	0.228 (-288.4)
5-P2-X	0.627 (-202.9)	0.735 (2.625)	0.462 (-135.4)
6-P4-Y	0.822 (2.2)	0.857 (0.277)	0.830 (-1.2)
6-P4-X	0.101 (-289.4)	0.057 (189.5)	0.098 (-113.0)
6-P3-Y	1.000 (0.0)	1.000 (0.0)	1.000 (0.0)
6-P3-X	0.157 (49.5)	0.046 (204.2)	0.127 (-93.4)
6-P2-Y	0.038 (-141.9)	0.025(159.1)	0.034 (-214.5)
6-P2-X	0.008 (13.5)	0.002 (232.6)	0.005 (-63.5)

Figure 9: Magnitude and phase (Deg.), of mode shapes (ARV)

Mode	A: Mag. (Phase)	B: Mag. (Phase)	C: Mag. (Phase)
1-P4-Y	1.000 (0.0)	1.000 (0.0)	1.000 (0.0)
1-P4-X	0.147 (173.3)	0.085 (128.5)	0.027 (163.7))
1-P3-Y	0.375 (-0.2)	0.378 (-0.2)	0.372 (-0.2)
1-P3-X	0.046 (172.1)	0.029 (103.8)	0.003 (53.7)
1-P2-Y	0.099 (180.8)	0.097 (-181.1)	0.096 (180.1)
1-P2-X	0.009 (167.3)	0.006 (111.7)	0.001 (46.9)
2-P4-Y	0.074 (-40.1)	0.037 (-17.7)	0.095 (4.0)
2-P4-X	1.000 (0.0)	1.000 (0.0)	1.000 (0.0)
2-P3-Y	0.021 (-6.3)	0.004 (-60.4)	0.022 (6.9)
2-P3-X	0.398 (-0.279)	0.397 (-0.3)	0.398 (-0.3)
2-P2-Y	0.007 (126.6)	0.002 (-221.8)	0.008 (182.1)
2-P2-X	0.089 (-1.7)	0.090 (-1.3)	0.089 (-1.3)
3-P4-Y	1.000 (0.0)	0.916 (-14.2)	0.980 (-7.5)
3-P4-X	0.344 (-181.6)	0.147 (36.5)	0.115 (-188.7)
3-P3-Y	0.927 (-4.5)	1.000 (0.0)	1.000 (0.0)
3-P3-X	0.143 (-189.1)	0.050 (16.1)	0.065 (-198.5)
3-P2-Y	0.476 (-183.4)	0.639 (177.8)	0.586 (-174.1)
3-P2-X	0.064 (-194.5)	0.013 (180.4)	0.034 (-189.2)
4-P4-Y	1.000 (0.0)	1.000 (0.0)	1.000 (0.0)
4-P4-X	0.094 (116.7)	0.108 (143.5)	0.378 (-263.5)
4-P3-Y	0.412 (221.7)	0.195 (188.6)	0.164(-198.3)
4-P3-X	0.200 (85.7)	0.064 (44.2)	0.071 (-190.6)
4-P2-Y	0.524 (21.7)	0.369 (-0.7)	0.423 (0.2)
4-P2-X	0.104 (110.5)	0.029 (4.8)	0.111(-115.2)
5-P4-Y	1.000 (0.0)	0.235 (-290.9)	0.686 (-86.6)
5-P4-X	0.942 (-273.5)	1.000 (0.0)	1.000 (0.0)
5-P3-Y	0.022 (-141.1)	0.048 (21.4)	0.061 (77.2)
5-P3-X	0.301 (-171.8)	0.376(-168.0)	0.571 (217.4)
5-P2-Y	0.412 (-0.8)	0.082 (-205.8)	0.296 (-102.8)
5-P2-X	0.474 (-118.7)	0.583(-176.2)	0.879 (201.6)
6-P4-Y	0.822 (-6.9)	0.851 (0.2)	0.836 (-8.5)
6-P4-X	0.185 (-93.7)	0.084 (185.3)	0.064 (93.7)
6-P3-Y	1.000 (0.0)	1.000 (0.0)	1.000 (0.0)
6-P3-X	0.067 (-76.5)	0.076 (194.2)	0.066 (72.0)
6-P2-Y	0.035 (-207.9)	0.027 (158.5)	0.029 (-127.6)
6-P2-X	0.015 (-46.1)	0.003 (239.8)	0.001 (10.1)

Figure 10: Magnitude and phase (Deg.) of mode shapes (ARMAV)

The estimated natural frequencies and damping ratios presented in figures 7 and 8, respectively, show only a slightly deviation between the two identification approaches. However, the damping ratios are generally lower for the ARV model than for the ARMAV model. The figures also show that the results for modes 4 and 5, respectively, are not as stable as the three other modes. It can also be seen from the stabilization diagrams.
The mode shape results shown in figures 9 and 10, respectively, also show that the results for modes 4 and 5 are not so reliable as those obtained for the other modes. The results for modes 1,2 and 6, respectively are very well identified for all the three recording periods. Modes 1 and 6 are seen to be bending modes close to the Y-direction while mode 2 is a bending mode close to the X-direction. Modes 4 and 5 which are more unstable seem to be bending modes in Y-direction and X-direction, respectively. Mode 3 is the first torsional mode about the vertical axis which is found by investigating the time series from the angular accelerometer about the the vertical axis. A closer investigation of how complex mode shapes can be interpreted as damped mode shapes could be done as proposed in Hoen [12]. It is shown that the damped mode shapes at an arbitrary position of a structure may be described by the product of an exponentially decaying function and an ellipse. In Hoen [12] the Gullfaks C structure has also been identified using a Markow Block Hankel matrix factorization method. The results from this paper and Hoen [12] correspond very well.

4 CONCLUSIONS

This paper has considered use of the multivariate ARMAV and ARV models for system identification of an offshore structure under natural random excitation. The estimated natural frequencies, damping ratios and mode shapes show only a slightly deviation between the two identification approaches. However, the damping ratios are generally lower for the ARV model than for the ARMAV model. Further, the ARMAV model also seems to give more stable mode shapes estimates for higher modes.

ACKNOWLEDGEMENT

The authors which to acknowledge Professor Ivar langen, Høgskolen i Stavanger, Norway for his kind release of information and data from the Gullfaks C platform.

5. REFERENCES

[1] Ljung, L.: System Identification: Theory for the User. Prentice Hall, Englewood Cliffs, 1987.

[2] Söderström, T. & P. Stoica: System Identification.Prentice-Hall, 1989.

[3] Davies, P., & J. K. Hammond: A Comparison of Fourier and Parametric Methods for Structural System Identification. Journal of Vibration, Acoustics, Stress and Reliability in Design. Vol. 106, pp.40-48, 1984.

[4] Gersch, W. & R. Liu: Time Series Methods for the Synthesis of Random Vibration Systems. ASME Transactions, Journal of Applied Mechanics, Vol. 98, No. 2, 1976.

[5] Pandit, S. W. & N. P. Metha: Data Dependent Systems Approach to Modal Analysis Via State Space. ASME paper No. 85-WA/DSC-1, 1985.

[6] Hac, A. & P. Spanos: Time Domain Structural Parameters Identification. Proc. of the Session of Structural Congress 87 (J. M. Roesset, ed.), 1987.

[7] Kozin,F. & H. G. Natke: System Identification Techniques. Structural Safety, Vol. 3, 1986.

[8] Jensen, J. L.: System Identification of Offshore Platforms. Ph.D-thesis, Aalborg University, 1990.

[9] Safak, E.: Identification of Linear Structures using Discrete-Time Filters. Journal of Structural Engineering, Vol. 117, No. 10, 1991.

[10] Hamamonto, T. & I. Kondo: Preliminary Experiment for Damage Detection of Offshore Structures. Proc. of the Third Int. Offshore and Polar Engineering Conference, Singapore, 1993.

[11] Li, C.-S., R.-J. Shyu, W.-J. Ko & H.-T. Lin: Multichannel Vibration Time Series Analysis of an Offshore Structural Model. J. CSME, Vol. 14, No. 1, 1993.

[12] Hoen, C.: System Identification of Structures Excited by Stochastic Load Processes. Dr.Ing. Thesis 1991:37, Division of Marine Structures, The Norwegian Institute of Technology, Trondheim, Norway, 1991.

[13] Langen, I & E. Skomedal : Measured and Predicted dynamic behaviour of the Gullfaks C gravity Platform. Proc. Of Behaviour of Offshore Structures, BOSS 92, London, 1992.

[14] Prevosto, M., M. Olagnon, A. Benveniste, M. Basseville & G. L. Vey : State Space Formulation: A solution to Modal Parameter Estimation. Journal of Sound and Vibration, Vol. 148, No. 2, pp. 329-342, 1991.

[15] Pi, Y. L. & N.C. Mickleborough: Modal Identification of Vibrating Structures using ARMA models. Journal og Engineering Mechanics, Vol. 115, No. 10, pp. 2232-2250, 1990

[16] Pimobo, B., E. Giorcelli, L. Garibaldi & A. Fasana: Structures Identification using ARMAV Models. Proc. of the IMAC XI Conf., Orlando, 1995.

[17] Andersen, P., R. Brincker & P.H. Kirkegaard : Theory of Covariance Equivalent ARMAV Models of Civil Eingineering Structures. Proc. of the IMAC XIV Conf., Dearborn, 1995.

[18] PC-MATLAB for MS-DOS Personal Computers, The Math Works, Inc., 1989.

[19] Myrvoll, F. : Instrumentation of the Skirt Piled Gullfaks C Gravity Platform for Performance Monitoring. Proc. Of Behaviour of Offshore Structures, BOSS 92, London, 1992.

FRACTURE AND DYNAMICS PAPERS

PAPER NO. 41: P. H. Kirkegaard & A. Rytter: *Use of a Neural Network for Damage Detection and Location in a Steel Member.* ISSN 0902-7513 R9245

PAPER NO. 42: L. Gansted: *Analysis and Description of High-Cycle Stochastic Fatigue in Steel.* Ph.D.-Thesis. ISSN 0902-7513 R9135.

PAPER NO. 43: M. Krawczuk: *A New Finite Element for Static and Dynamic Analysis of Cracked Composite Beams.* ISSN 0902-7513 R9305.

PAPER NO. 44: A. Rytter: *Vibrational Based Inspection of Civil Engineering Structures.* Ph.D.-Thesis. ISSN 0902-7513 R9314.

PAPER NO. 45: P. H. Kirkegaard & A. Rytter: *An Experimental Study of the Modal Parameters of a Damaged Steel Mast.* ISSN 0902-7513 R9320.

PAPER NO. 46: P. H. Kirkegaard & A. Rytter: *An Experimental Study of a Steel Lattice Mast under Natural Excitation.* ISSN 0902-7513 R9326.

PAPER NO. 47: P. H. Kirkegaard & A. Rytter: *Use of Neural Networks for Damage Assessment in a Steel Mast.* ISSN 0902-7513 R9340.

PAPER NO. 48: R. Brincker, M. Demosthenous & G. C. Manos: *Estimation of the Coefficient of Restitution of Rocking Systems by the Random Decrement Technique.* ISSN 0902-7513 R9341.

PAPER NO. 49: L. Gansted: *Fatigue of Steel: Constant-Amplitude Load on CCT-Specimens.* ISSN 0902-7513 R9344.

PAPER NO. 50: P. H. Kirkegaard & A. Rytter: *Vibration Based Damage Assessment of a Cantilever using a Neural Network.* ISSN 0902-7513 R9345.

PAPER NO. 51: J. P. Ulfkjær, O. Hededal, I. B. Kroon & R. Brincker: *Simple Application of Fictitious Crack Model in Reinforced Concrete Beams.* ISSN 0902-7513 R9349.

PAPER NO. 52: J. P. Ulfkjær, O. Hededal, I. B. Kroon & R. Brincker: *Simple Application of Fictitious Crack Model in Reinforced Concrete Beams. Analysis and Experiments.* ISSN 0902-7513 R9350.

PAPER NO. 53: P. H. Kirkegaard & A. Rytter: *Vibration Based Damage Assessment of Civil Engineering Structures using Neural Networks.* ISSN 0902-7513 R9408.

PAPER NO. 54: L. Gansted, R. Brincker & L. Pilegaard Hansen: *The Fracture Mechanical Markov Chain Fatigue Model Compared with Empirical Data.* ISSN 0902-7513 R9431.

PAPER NO. 55: P. H. Kirkegaard, S. R. K. Nielsen & H. I. Hansen: *Identification of Non-Linear Structures using Recurrent Neural Networks.* ISSN 0902-7513 R9432.

PAPER NO. 56: R. Brincker, P. H. Kirkegaard, P. Andersen & M. E. Martinez: *Damage Detection in an Offshore Structure.* ISSN 0902-7513 R9434.

PAPER NO. 57: P. H. Kirkegaard, S. R. K. Nielsen & H. I. Hansen: *Structural Identification by Extended Kalman Filtering and a Recurrent Neural Network.* ISSN 0902-7513 R9433.

FRACTURE AND DYNAMICS PAPERS

PAPER NO. 58: P. Andersen, R. Brincker, P. H. Kirkegaard: *On the Uncertainty of Identification of Civil Engineering Structures using ARMA Models.* ISSN 0902-7513 R9437.

PAPER NO. 59: P. H. Kirkegaard & A. Rytter: *A Comparative Study of Three Vibration Based Damage Assessment Techniques.* ISSN 0902-7513 R9435.

PAPER NO. 60: P. H. Kirkegaard, J. C. Asmussen, P. Andersen & R. Brincker: *An Experimental Study of an Offshore Platform.* ISSN 0902-7513 R9441.

PAPER NO. 61: R. Brincker, P. Andersen, P. H. Kirkegaard, J. P. Ulfkjær: *Damage Detection in Laboratory Concrete Beams.* ISSN 0902-7513 R9458.

PAPER NO. 62: R. Brincker, J. Simonsen, W. Hansen: *Some Aspects of Formation of Cracks in FRC with Main Reinforcement.* ISSN 0902-7513 R9506.

PAPER NO. 63: R. Brincker, J. P. Ulfkjær, P. Adamsen, L. Langvad, R. Toft: *Analytical Model for Hook Anchor Pull-out.* ISSN 0902-7513 R9511.

PAPER NO. 64: P. S. Skjærbæk, S. R. K. Nielsen, A. Ş. Çakmak: *Assessment of Damage in Seismically Excited RC-Structures from a Single Measured Response.* ISSN 1395-7953 R9528.

PAPER NO. 65: J. C. Asmussen, S. R. Ibrahim, R. Brincker: *Random Decrement and Regression Analysis of Traffic Responses of Bridges.* ISSN 1395-7953 R9529.

PAPER NO. 66: R. Brincker, P. Andersen, M. E. Martinez, F. Tallavó: *Modal Analysis of an Offshore Platform using Two Different ARMA Approaches.* ISSN 1395-7953 R9531.

PAPER NO. 67: J. C. Asmussen, R. Brincker: *Estimation of Frequency Response Functions by Random Decrement.* ISSN 1395-7953 R9532.

PAPER NO. 68: P. H. Kirkegaard, P. Andersen, R. Brincker: *Identification of an Equivalent Linear Model for a Non-Linear Time-Variant RC-Structure.* ISSN 1395-7953 R9533.

PAPER NO. 69: P. H. Kirkegaard, P. Andersen, R. Brincker: *Identification of the Skirt Piled Gullfaks C Gravity Platform using ARMAV Models.* ISSN 1395-7953 R9534.

PAPER NO. 70: P. H. Kirkegaard, P. Andersen, R. Brincker: *Identification of Civil Engineering Structures using Multivariate ARMAV and RARMAV Models.* ISSN 1395-7953 R9535.

PAPER NO. 71: P. Andersen, R. Brincker, P. H. Kirkegaard: *Theory of Covariance Equivalent ARMAV Models of Civil Engineering Structures.* ISSN 1395-7953 R9536.

Department of Building Technology and Structural Engineering
Aalborg University, Sohngaardsholmsvej 57, DK 9000 Aalborg
Telephone: +45 98 15 85 22 Telefax: +45 98 14 82 43